Line Parameters for $^{16}O_3$ Bands in the 7 μm Region

J.-M. Flaud and C. Camy-Peyret

Laboratoire de Physique Moléculaire et Atmosphérique

Tour 13, 3e etage

Université Pierre et Marie Curie et C.N.R.S.

4 place Jussieu

75252 Paris Cedex 05

France

C. P. Rinsland and M. A. H. Smith

NASA Langley Research Center

Atmospheric Sciences Division

Mail Stop 401A

Hampton, Virginia 23665-5225

U. S. A.

V. Malathy Devi

College of William and Mary

Physics Department

Williamsburg, Virginia 23185

U. S. A.

Manuscript pages: 19
Figures: 2
Tables: 1

Running title: $^{16}O_3$ Bands near 7.1 μm

Mail correspondence to:

Dr. Jean-Marie Flaud

Laboratoire de Physique Moléculaire et Atmosphérique

Tour 13, 3^{e} etage

Université Pierre et Marie Curie et C.N.R.S.

4 place Jussieu

75252 Paris Cedex 05

France

ABSTRACT

Lines of the very weak $2\nu_2$ and $\nu_1 + \nu_3 - \nu_2$ bands of $^{16}O_3$ have been identified in the 1370 to 1440 cm^{-1} region of 0.01-cm^{-1} resolution solar occultation spectra of the stratosphere. The spectral data were acquired from orbit by the Atmospheric Trace Molecule Spectroscopy (ATMOS) Fourier transform spectrometer during the Spacelab 3 shuttle mission. Initial assignments for the lines were obtained using positions calculated from accurate molecular constants derived in recent high resolution laboratory studies. From these results and spectral simulations of the interfering atmospheric absorptions, 59 $^{16}O_3$ lines in the atmospheric spectra were selected for intensity measurements using the equivalent width technique. Precise transition moment constants for both bands were then deduced from the measured intensities and used with the molecular constants to generate a complete listing of line positions, intensities, and lower state energies useful for atmospheric applications. The integrated band intensities in units of cm^{-1}/molecule cm^{-2} at 296 K are 5.43×10^{-22} for the $2\nu_2$ band and 1.01×10^{-21} for the $\nu_1 + \nu_3 - \nu_2$ band.

INTRODUCTION

Because of the atmospheric importance of ozone, the spectrum of $^{16}O_3$ and those of the less terrestrially abundant isotopic species have been the subject of a number of recent high-resolution investigations in the microwave and infrared regions (Refs. 1-11). The infrared work on $^{16}O_3$ has covered the regions of all of the major vibration-rotation bands down to 4.8 μm: ν_2 (14.2 μm) (2), ν_3 and ν_1 (10 μm) (3, 4), $\nu_1 + \nu_2$ and $\nu_2 + \nu_3$ (5.7 μm) (5), and $2\nu_1$, $2\nu_3$, and $\nu_1 + \nu_3$ (4.8 μm) (11). However, weak absorption by ozone is also known to occur near 7.1 μm. This absorption was first measured at low resolution by McCaa and Shaw (12) and assigned to the $2\nu_2$ band. The long-path, low-pressure ozone laboratory atlas of Damon et al. (13) shows this absorption at a resolution of about 0.04 cm^{-1}. More recently, O_3 absorption features have been observed between 1380 and 1430 cm^{-1} in 0.02 cm^{-1} resolution balloon-borne solar occultation spectra of the stratosphere. These results have been reported in the September 1986 and September 1987 updates (14) to an atlas containing the observed spectra and measured line positions (15).

In this work, we report the analysis of O_3 absorption features in the 1370 to 1440 cm^{-1} region of 0.01 cm^{-1} resolution solar occultation spectra of the lower stratosphere. Individual lines of the $2\nu_2$ and $\nu_1 + \nu_3 - \nu_2$ bands of $^{16}O_3$ have been identified using positions calculated from vibrational energies, rotational and coupling constants based on previous investigations (2, 4, 11). Intensities of 59 $^{16}O_3$ lines measured from the solar spectra have been fitted to derive accurate transition moment constants for both bands. A complete listing of line positions, intensities, and lower state energies has been generated.

OBSERVATIONAL DATA

The spectral data used in our analysis were acquired from orbit by the ATMOS (Atmospheric Trace Molecule Spectroscopy) instrument, a high-speed Fourier transform spectrometer designed to obtain measurements of the Earth's upper atmosphere through high-resolution solar occultation observations covering the 2 to 16 μm region. The spectral measurements were recorded on April 30-May 1, 1985, during the Spacelab 3 mission. Details concerning the ATMOS instrument and its operation during Spacelab 3 are described by Farmer and Raper (16) and Farmer et al. (17).

The basic components of the ATMOS instrument are a double-passed Michelson interferometer, a telescope, and a hemispherical Sun tracker. During each occultation, the interferometer records double-sided interferograms every 2.2 s which, from the Spacelab 3 orbital altitude of 360 km, corresponds to successive tangent height separations of about 4.2 km in the upper atmosphere. In the lower stratosphere and troposphere, the spacing between tangent heights of successive scans is reduced by refraction and by drifts of the Sun tracker field of view on the "flattened" solar disk. The maximum path difference of each scan is 47.5 cm, yielding an unapodized spectral resolution of about 0.01 cm^{-1}. The radiation is detected by a HgCdTe detector cooled to 77 K.

ATMOS spectra are derived from the inverse Fourier transform of two-sided interferograms with the same central fringe measurement. The intensities at each wavenumber in the "low Sun" (atmospheric) spectra are subsequently ratioed to the corresponding value in a high Sun (exo-atmospheric) spectrum to eliminate solar features and to remove the wavelength dependence of the instrumental response and the solar flux. Processing of the ATMOS spectra and the analysis software will be described in a future publication (18). Tangent

pressures of the individual spectra have been determined by spectral fitting suitable temperature-independent absorption lines of atmospheric constituents whose volume mixing ratios are well known (e.g. CO_2 and N_2). Details concerning the retrieval of pressure-temperature profiles from the ATMOS spectra will be described elsewhere (19).

Because O_3 absorption is very weak in the 7.1 μm region, it is important to use spectral data with the highest possible signal-to-noise ratio and maximum O_3 absorption. For this reason, we analyzed a single spectrum obtained by coadding 3 ratio spectra with the strongest O_3 lines. These spectra are from ATMOS occultations SS03, SS07, and SS12 (SS=sunset) and were recorded with a filter covering approximately 1100 to 2000 cm^{-1}. The latitudes and tangent heights of the individual spectra ranged from 25.9°N to 32.3°N and 22.0 and 23.5 km, respectively. The effective tangent height of the coadded spectrum is 22.8 km, corresponding to a tangent pressure of 35.7 mbar. The resulting spectrum has been apodized with the moderate (number 2) apodizing function of Norton and Beer (20) to reduce the sidelobes of the interferometer response function. The signal-to-rms noise ratio of the coadded spectrum is about 400 near 1400 cm^{-1}. The O_3 absorption features are very weak with line center absorption depths of about 5% or less.

RESULTS

A. Line Positions

The rotational energy levels of the (101) vibrational state were calculated using the vibrational energy, and the rotational and coupling constants quoted in Ref. 11. In order to be consistent with the ground state rotational energy levels obtained in Ref. 4 and already used extensively in our previous

works on $^{16}O_3$ (4, 5, 11), we have refitted the data on the ν_2 and $2\nu_2 - \nu_2$ bands as well as the pure rotation transitions in (010) and (020) given in Ref. 2. The constants deduced for the corresponding vibrational states are given in Table I. Finally with these spectroscopic constants available, the line positions of the $2\nu_2$ and $\nu_1 + \nu_3 - \nu_2$ bands were derived from the calculated energy levels.

B. Line Intensities

The equivalent width technique has been used to derive line intensities from the ATMOS spectra. Selection of the lines for measurement was based on the predicted line positions and on comparisons of the ATMOS spectra with synthetic spectra computed with all known absorbing atmospheric gases other than O_3. The simulations were generated assuming the spectroscopic parameters on the ATMOS line list (21) and vertical volume mixing ratio profiles retrieved from analysis of the individual spectra from the same occultations (22). The primary interfering atmospheric gases in this region are H_2O and CH_4. Using these criteria, 27 lines of O_3 in the $2\nu_2$ band up to J = 37 and K_a = 8 and 32 lines in the $\nu_1 + \nu_3 - \nu_2$ band up to J = 24 and K_a = 11 were measured.

Intensities were derived by matching the measured equivalent widths with values calculated for the same integration interval. In these calculations, we assumed the average of the O_3 vertical volume mixing ratio profiles retrieved for occultations SS03, SS07, and SS12 using O_3 lines appearing in the 10-μm region, along with a Voigt line shape and an air-broadened half-width of 0.075 $cm^{-1}atm^{-1}$ at 296 K for all lines. The temperature dependence of the half-width was modeled using the usual power law

$(296/T)^{-n}$ with n = 0.75. Corrections for nonzero wing absorption in the intervals used to define the 100% transmission level were included. The O_3 parameters used to retrieve the O_3 vertical profiles are from Ref. 4; hence, the present intensities are consistent with the intensities in the 10-μm region (ν_1, ν_3) (Ref. 4), the 5.7-μm region ($\nu_1 + \nu_2$, $\nu_2 + \nu_3$) (Ref. 5), and the 4.8-μm region ($2\nu_1$, $2\nu_3$, $\nu_1 + \nu_3$) (Ref. 11).

The experimental intensities were then reproduced using the transition moment operators expanded as follows:

$$(000)(020)_{\mu_Z}' = (-0.7870 \pm 0.0040)\times10^{-3}\ \phi_X + (0.1720 \pm 0.0089)\times10^{-4}\{i\phi_y, J_z\} + (0.1810 \pm 0.0012)\times10^{-4}\{\phi_z, iJ_y\} \quad (1)$$

$$(101)(010)_{\mu_Z}' = (-0.7839 \pm 0.0098)\times10^{-2}\ \phi_Z + (0.154 \pm 0.072)\times10^{-4}\ 1/2\ (\{\phi_x, iJ_y\} - \{i\phi_y, J_x\}) \quad (2)$$

Using the calculated energy levels together with the transition moment operators listed in Eqs. (1) and (2), we have generated a list of 2535 line positions, intensities, and lower state energies for the $2\nu_2$ and $\nu_1 + \nu_3 - \nu_2$ bands of $^{16}O_3$. The calculations were performed using a partition function Z(296 K) = 3473 and an intensity cutoff of 0.1×10^{-24} cm^{-1}/molecule cm^{-2} at 296 K, with maximum values of 55 for J and 13 for K_a. Total band intensities of 0.543×10^{-21} and 0.101×10^{-20} cm^{-1}/molecule cm^{-2} at 296 K were obtained respectively for the $2\nu_2$ and $\nu_1 + \nu_3 - \nu_2$ bands of $^{16}O_3$. No previous intensity measurements have been reported for these bands.

Figures 1 and 2 show comparisons of the ATMOS and calculated spectra in two different narrow spectral intervals. In all cases, the measured features

of the $2\nu_2$ and $\nu_1 + \nu_3 - \nu_2$ bands are reproduced very well by the calculations. There are a number of very weak unassigned absorption lines occuring in the 1370 to 1440 cm^{-1} region, for example, the feature marked by "?" in Fig. 2, indicating the need for further improvement in the line parameters for this interval.

Using the constants in our Table I and in Ref. (11), a listing of line parameters for the $2\nu_1 - \nu_2$ and $2\nu_3 - \nu_2$ bands of $^{16}O_3$ was also generated. Although a few coincidences between the predicted lines and unidentified weak features were noted, it was not possible to unambiguously identify either band in the ATMOS spectra.

Finally, it should be emphasized that the absolute intensities calculated here for the $2\nu_2$ and $\nu_1 + \nu_3 - \nu_2$ bands have been calibrated against the intensities for the ν_3 and ν_1 bands in the 10-μm region (4) which have been obtained assuming the value of $(\partial\mu_Z/\partial q_3)_e$ = -0.2662 D (see Ref. 4). If this value is to be changed, all of the intensities reported in this study and in Refs. (4, 5, 11) will have to be multiplied by the square of the ratio of the $(\partial\mu_Z/\partial q_3)_e$ values (modified divided by the Ref. 4 value). The line parameters computed in this study will be made available for inclusion in updates to the ATMOS linelist (21) and the HITRAN (high-resolution transmission molecular absorption) database (23).

TABLE I

Vibrational energies and rotational constants in cm^{-1} for the (010) and (020) vibrational states of $^{16}O_3$

	v=(010)		v=(020)	
E_v	700.931056	± 0.000017	1399.27263	± 0.00005
A^v	3.60709296_{60}	± 0.00000032	3.6624061_{84}	± 0.0000014
B^v	0.444021809_{42}	± 0.000000041	0.44274468_{90}	± 0.00000016
C^v	0.392439113_{18}	± 0.000000038	0.39007213_{99}	± 0.00000014
Δ_K^v	$(0.2327460_{64}$	± 0.0000065)x10^{-3}	$(0.256077_{05}$	± 0.000083)x10^{-3}
Δ_{JK}^v	$(-0.179003_{89}$	± 0.000056)x10^{-5}	$(-0.17211_{88}$	± 0.00038)x10^{-5}
Δ_J^v	$(0.457106_{09}$	± 0.000032)x10^{-6}	$(0.46006_{38}$	± 0.00019)x10^{-6}
δ_K^v	$(0.38893_{83}$	± 0.00010)x10^{-5}	$(0.45899_{45}$	± 0.00087)x10^{-5}
δ_J^v	$(0.692601_{09}$	± 0.000040)x10^{-7}	$(0.68636_{32}$	± 0.00043)x10^{-7}
H_K^v	$(0.48866_{16}$	± 0.00069)x10^{-7}	$(0.610_{16}$	± 0.014)x10^{-7}
H_{KJ}^v	$(-0.21209_{22}$	± 0.00057)x10^{-8}	$(-0.2541_{86}$	± 0.0066)x10^{-8}
H_{JK}^v	$(0.308_{85}$	± 0.071)x10^{-11}	$(0.185_{85}$	± 0.096)x10^{-10}
H_J^v	$(0.3136_{70}$	± 0.0070)x10^{-12}	$(0.118_{45}$	± 0.069)x10^{-12}
h_K^v	$(0.3196_{78}$	± 0.0053)x10^{-8}	$(0.477_{90}$	± 0.073)x10^{-8}
h_{KJ}^v	$(-0.1154_{89}$	± 0.0058)x10^{-10}	$(-0.26_{78}$	± 0.10)x10^{-10}

h_J^v	$(0.1868_{49}$	$\pm 0.0016)\times10^{-12}$	$(0.238_{24}$	$\pm 0.036)\times10^{-12}$
L_K^v	$(-0.1581_{88}$	$\pm 0.0029)\times10^{-10}$	$(-0.338_{46}$	$\pm 0.093)\times10^{-10}$
L_{KKJ}^v	$(0.479_{84}$	$\pm 0.014)\times10^{-12}$		
l_K^v	$(0.636_{32}$	$\pm 0.075)\times10^{-12}$	$(-0.95_{30}$	$\pm 0.29)\times10^{-12}$
l_{KJ}^v	$(0.382_{97}$	$\pm 0.018)\times10^{-12}$		
P_K^v	$(0.498_{03}$	$\pm 0.040)\times10^{-14}$	$(0.40_{10}$	$\pm 0.20)\times10^{-12}$

References

1. M. Carlotti, G. Di Lonardo, L. Fusina, A. Trombetti, A. Bonetti, B. Carli, and F. Mencaraglia, J. Mol. Spectrosc. 107, 84-93 (1984).
2. H. M. Pickett, E. A. Cohen, L. R. Brown, C. P. Rinsland, M. A. H. Smith, V. Malathy Devi, A. Goldman, A. Barbe, B. Carli, and M. Carlotti, J. Mol. Spectrosc. 128, 151-171, 1988.
3. H. M. Pickett, E. A. Cohen, and J. Margolis, J. Mol. Spectrosc. 110, 186-214 (1985).
4. J.-M. Flaud, C. Camy-Peyret, V. Malathy Devi, C. P. Rinsland, and M. A. H. Smith, J. Mol. Spectrosc. 124, 209-217 (1987).
5. V. Malathy Devi, J.-M. Flaud, C. Camy-Peyret, C. P. Rinsland, and M. A. H. Smith, J. Mol. Spectrosc. 125, 174-183 (1987).
6. C. Chiu and E. A. Cohen, J. Mol. Spectrosc. 109, 239-245 (1985).
7. C. Camy-Peyret, J.-M. Flaud, A. Perrin, V. Malathy Devi, C. P. Rinsland, and M. A. H. Smith, J. Mol. Spectrosc. 118, 345-354 (1986).
8. J.-M. Flaud, C. Camy-Peyret, V. Malathy Devi, C. P. Rinsland, and M. A. H. Smith, J. Mol. Spectrosc. 118, 334-344 (1986).
9. C. P. Rinsland, V. Malathy Devi, J.-M. Flaud, C. Camy-Peyret, M. A. H. Smith, and G. M. Stokes, J. Geophys. Res. 90, 10719-10725 (1985).
10. J.-M. Flaud, C. Camy-Peyret, V. Malathy Devi, C. P. Rinsland, and M. A. H. Smith, J. Mol. Spectrosc. 122, 221-228 (1987).
11. C. P. Rinsland, M. A. H. Smith, J.-M. Flaud, C. Camy-Peyret, and V. Malathy Devi, J. Mol. Spectrosc. 130, 204-212, 1988.
12. D. J. McCaa and J. H. Shaw, J. Mol. Spectrosc. 25, 374-397 (1968).
13. E. Damon, R. L. Hawkins, and J. H. Shaw, unpublished results.

14. A. Goldman, R. D. Blatherwick, F. J. Murcray, J. W. VanAllen, F. H. Murcray, and D. G. Murcray, unpublished results.

15. A. Goldman, R. D. Blatherwick, F. J. Murcray, J. W. VanAllen, F. H. Murcray, and D. G. Murcray, Appl. Opt. 21, 1163-1164 (1982).

16. C. B. Farmer and O. F. Raper, NASA Conference Proceedings CP-2429 (1986).

17. C. B. Farmer, O. F. Raper, and F. G. O'Callaghan, JPL Publication 87-32, 45 pp. (1987).

18. R. H. Norton, private communication.

19. C. B. Farmer, private communication.

20. R. H. Norton and R. Beer, J. Opt. Soc. Am. 66, 259-264 (1976).

21. L. R. Brown, C. B. Farmer, C. P. Rinsland, and R. A. Toth, Appl. Opt. 26, 5154-5182 (1987).

22. M. R. Gunson, C. B. Farmer, R. H. Norton, R. Zander, C. P. Rinsland, J. H. Shaw, B.-C. Gao, and J. Namkung, unpublished results.

23. L. S. Rothman, R. R. Gamache, A. Goldman, L. R. Brown, R. A. Toth, H. M. Pickett, R. L. Poynter, J.-M. Flaud, C. Camy-Peyret, A. Barbe, N. Husson, C. P. Rinsland, and M. A. H. Smith, Appl. Opt. 26, 4058-4097 (1987).

Acknowledgments

We thank Crofton B. Farmer, the ATMOS principal investigator, for his encouragement and for permission to employ the ATMOS Spacelab 3 data base for this study. We also wish to acknowledge the assistance provided by Robert H. Norton, Susan Paradise, and others at the Jet Propulsion Laboratory in enabling us to access the ATMOS spectra. The authors also thank Susan Edwards of NASA Langley for her help in preparing this manuscript. Research at the College of William and Mary was supported under Cooperative Agreement NCC1-80 with NASA.

FIGURE CAPTIONS

Figure 1. ATMOS (solid line) and simulated (dotted line) spectra in a narrow interval containing a number of transitions of the $\nu_1 + \nu_3 - \nu_2$ and $2\nu_2$ bands of $^{16}O_3$. The measured intensities have been normalized to the highest value in the interval. Note the expanded vertical scaling of the plot; only the upper 4% of the spectrum is shown.

Figure 2. ATMOS (solid line) and simulated (dotted line) spectra in a narrow interval containing a number of R branch transitions of the $2\nu_2$ band of $^{16}O_3$. The measured intensities have been normalized to the highest value in the interval. Note the expanded vertical scaling of the plot; only the upper 30% of the spectrum is shown. Stratospheric lines of HDO and CH_4 are marked.

Figure 1

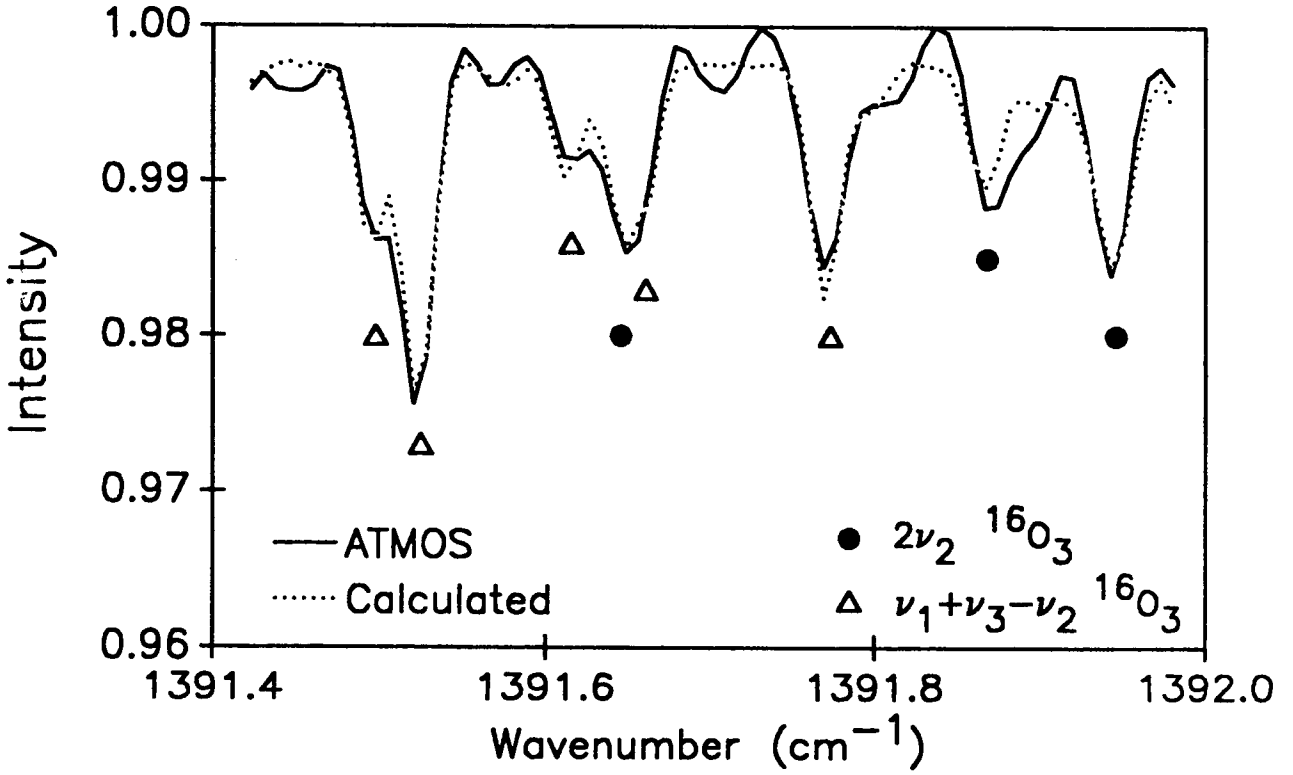
1.00
0.99
0.98
0.97
0.96
Intensity
ATMOS
Calculated
$2\nu_2$ $^{16}O_3$
$\nu_1+\nu_3-\nu_2$ $^{16}O_3$
1391.4
1391.6
1391.8
1392.0
Wavenumber (cm^{-1})

Figure 2

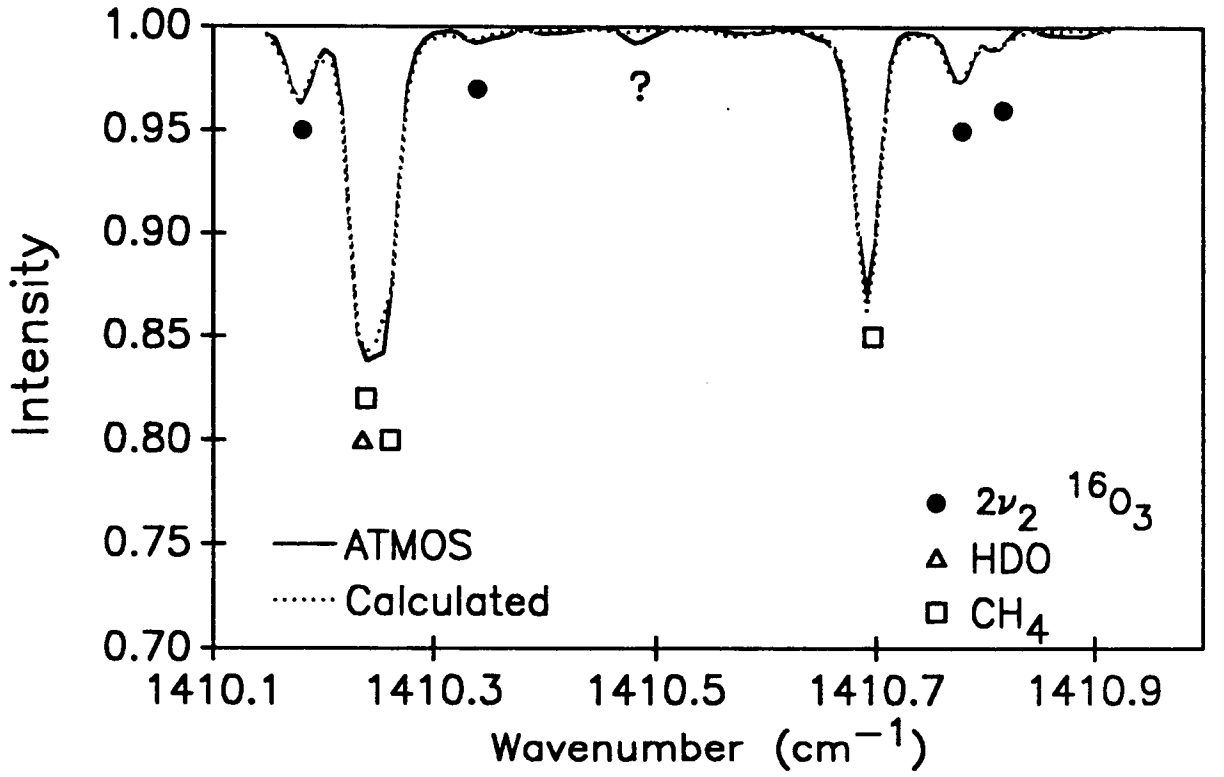
1.00
0.95
0.90
0.85
0.80
0.75
0.70
Intensity
?
ATMOS
Calculated
$2\nu_2$ $^{16}O_3$
HDO
CH_4
1410.1
1410.3
1410.5
1410.7
1410.9
Wavenumber (cm^{-1})

LIST OF TABLES

Table I. Vibrational energies and rotational constants for the (010) and (020) vibrational states of $^{16}O_3$.

LIST OF SYMBOLS

ν - lower case Greek nu

μ - lower case Greek mu

Δ - upper case Greek delta

δ - lower case Greek delta

ϕ - lower case Greek phi

∂ - symbol for partial derivative